Article published online: 2024-06-27

How Flow Diverter Selection Can Affect the Flow Changes within a Jailed Ophthalmic Artery: A Computational Fluid Dynamics Study

Can Ünsal[1] Görkem Güçlü[2] Ali Bahadir Olcay[3] Amir Hassankhani[4] Cem Bilgin[5] Bahattin Hakyemez[6]

[1] Numerical Simulation and Spray Targeting Division, Department of Engineering, Bosch, Bursa, Türkiye
[2] Department of Mechanical Engineering, Southern Methodist University, Dallas, Texas, United States
[3] Department of Mechanical Engineering, Faculty of Engineering, Yeditepe University, Istanbul, Türkiye
[4] Department of Radiology, Keck School of Medicine, University of Southern California, Los Angeles, California, United States
[5] Department of Radiology, Mayo Clinic, Rochester, Minnesota, United States
[6] Department of Radiology, Uludag University School of Medicine, Bursa, Türkiye

Address for correspondence Ali Bahadir Olcay, PhD, Department of Mechanical Engineering, Yeditepe University, İstanbul, Türkiye (e-mail: abolcay@gmail.com).

Asian J Neurosurg 2024;19:426–434.

Abstract

Introduction Flow diverter (FD) stents are widely used to treat giant aneurysms by reducing blood flow into the aneurysm sac. However, choosing the optimal FD for a patient can be challenging when a nearby artery, such as the ophthalmic artery (OA), is jailed by the FD placement. This study compares the impact of two FD stents with different effective metal surface area (EMSA) values on OA occlusion.

Materials and Methods A numerical model of a 59-year-old female patient with a giant aneurysm in the left internal carotid artery and a jailed OA was created based on clinical data. Two FD stents, FRED4017 and FRED4518, with different EMSA values at the aneurysm neck and OA inlet, were virtually deployed in the model. Blood flow and occlusion amount in the OA were simulated and compared between the two FD stents.

Results FRED4017 had higher EMSA values than FRED4518 at the aneurysm neck (35% vs. 24.6%) and lower EMSA values at the OA inlet (15% vs. 21.2%). FRED4017 caused more occlusion in the OA than FRED4518 (40% vs. 28%), indicating a higher risk of ocular ischemic syndrome.

Conclusion The EMSA value of FD stents affects the blood flow and occlusion amount in the jailed OA. Therefore, selecting an FD stent with a low EMSA value at the OA inlet may be beneficial for patients with a nearby jailed artery at the aneurysm neck.

Keywords
- cerebral aneurysm
- jailed artery
- ocular ischemic syndrome
- flow diverter stent
- patient-specific CFD modeling

article published online
June 27, 2024

DOI https://doi.org/10.1055/s-0044-1787868.
ISSN 2248-9614.

Thieme Medical and Scientific Publishers Pvt. Ltd., A-12, 2nd Floor, Sector 2, Noida-201301 UP, India

Introduction

Flow diverter (FD) stents guide blood flow in the aneurysm, carrying arteries to the parent artery, and creating resistance to blood entering the sac. Therefore, reducing the blood flow entering the aneurysm sac leads to thrombosis, and thus, aneurysmal occlusion begins. The feasibility of flow diversion has been demonstrated in different areas, such as anterior and posterior circulation aneurysms, iatrogenic internal carotid artery (ICA) injuries, and ruptured aneurysms.[1,2] Nevertheless, today, the most common indication for flow diversion is the giant, wide-necked ICA aneurysms.[1,3–8] In wide-necked ICA aneurysms, total occlusion rates vary between 62.8 and 76.8%[9] with flow diversion. However, it would not be prudent to evaluate the success of flow diversion only with aneurysm occlusion. Microsurgery or additional coiling can be employed as a rescue treatment in case of residual filling, whereas thromboembolic and hemorrhagic complications secondary to flow diversion may have fatal consequences. Unfortunately, currently, the rates of devastating complications, such as intracranial hemorrhage, stroke, and death, vary between 2.9 and 14% with flow diversion.[1,6,9–13]

Recent studies have underscored the prevalence and significance of ocular complications associated with flow diversion in the treatment of intracranial aneurysms. For instance, a comprehensive study indicated that, while flow diversion is a promising treatment for aneurysms causing compressive neuro-ophthalmologic symptoms, it carries a relevant risk for complications, including visual impairment, with morbidity and mortality rates of 7.4 and 3.7%, respectively.[14] Furthermore, an evaluation of ophthalmic artery (OA) aneurysms treated with flow diversion highlighted that, despite high rates of procedural success and patent ophthalmic arteries postprocedure, there were instances of transient peripheral vision loss potentially related to the procedure, underscoring the critical balance between therapeutic success and the risk of ocular complications.[15] Additionally, a longitudinal study on neurological complications following FD implantation for intracranial aneurysms revealed that ischemic events, including those potentially leading to visual outcomes, were a significant portion of postprocedural complications, emphasizing the need for careful patient selection and postoperative management.[16] These findings highlight the necessity of a nuanced approach to FD selection and deployment, especially in cases where ocular structures may be at risk, further supporting the urgency and relevance of the current study's research question.

Flow diversion primarily targets the aneurysm neck; nevertheless, implants may also cover the side branches of ICA, as in paraophthalmic aneurysms.[17–19] Today, rates of visual impairment after flow diversion range between 3 and 39.3%.[20,21] Furthermore, despite the studies on the clinical significance of OA coverage, the OA occlusion predictor variables are still unclear. Since a FD limits the blood flow entering the aneurysm sac based on its mesh density, pretreatment computational fluid dynamics (CFD) analysis can reveal velocity changes at the aneurysm neck region, including covered side branches. Therefore, in addition to predicting aneurysm occlusion, a pretreatment CFD analysis can also predict thromboembolic complications. With these advances, pretreatment CFD can guide the selection of the most beneficial FD not only for aneurysm treatments but also for nearby arteries to the aneurysm sacs; thus, it can be decisive for treatment success. In this study, we have numerically investigated an aneurysm-carrying artery and its nearby OA after placement of two FD stents to the aneurysm neck region to quantify reduced blood flow amount in the covered OA for the first time in the literature.

Materials and Methods

Developing a Patient-Specific Numerical Model

A 59-year-old female patient with an intermittent headache, which had exacerbated in the last 2 months, was accepted to the clinic for treatment. Cranial magnetic resonance (MR) imaging revealed a giant aneurysm in the ophthalmic segment of the patient's left ICA (LICA), as shown inside a red ellipse shape in ►**Fig. 1A**. Flow diversion was considered the first-line treatment because of the localization of the aneurysm. However, using an FD at the patient's aneurysm neck could have fully covered the OA, which might have caused a change of hemodynamics at the corresponding arteries, yielding a possibility of a stroke. Therefore, the FRED4518 FD stent, having a 29% effective metal surface area (EMSA), was decided to be implanted into the aneurysm site of the patient's LICA to provide healing of the patient's giant aneurysm and sufficient blood flow into OA by eliminating any possible rupture and stroke in the clinic.

Once a FRED4518 FD stent was placed into the patient's aneurysm site by the interventional radiologists in the clinic, angiographic images of the patient were received in Digital Imaging and Communications in Medicine format to be processed by 3D-Slicer (https://www.slicer.org/), Meshmixer (http://www.meshmixer.com/, Autodesk, Inc., San Rafael, California, United States), and SpaceClaim (ANSYS, Inc., Canonsburg, Pennsylvania, United States) to build a patient-specific fluid domain. ►**Fig. 1A** illustrates the location and size of the patient's aneurysm in the skull, while a digital subtraction angiography (DSA) image of the patient's aneurysm sac on a plane is shown in ►**Fig. 1B**. Lastly, a three-dimensional patient-specific fluid domain was created from the patient's DSA images given in ►**Fig. 1C** with neighbor arteries.

Virtual FD Stent Placement into the Patient's Aneurysm Site in LICA

Determination of the most convenient FD for an aneurysm neck can be challenging for interventional radiologists. Besides, the selection of FD can even be more dramatic when the FD has to cover a neighbor artery in addition to the aneurysm neck. Since the aneurysm of the patient in the clinic was treated with FRED4518, a total of 64-wire-braid FRED4518 with 48 wires of 22.5-µm diameters and 16 wires of 56-µm diameters were virtually knitted into the patient's aneurysm neck and OA entrance in the present study as shown in ►**Fig. 2A** and **B**. FRED4017 FD stent having the same

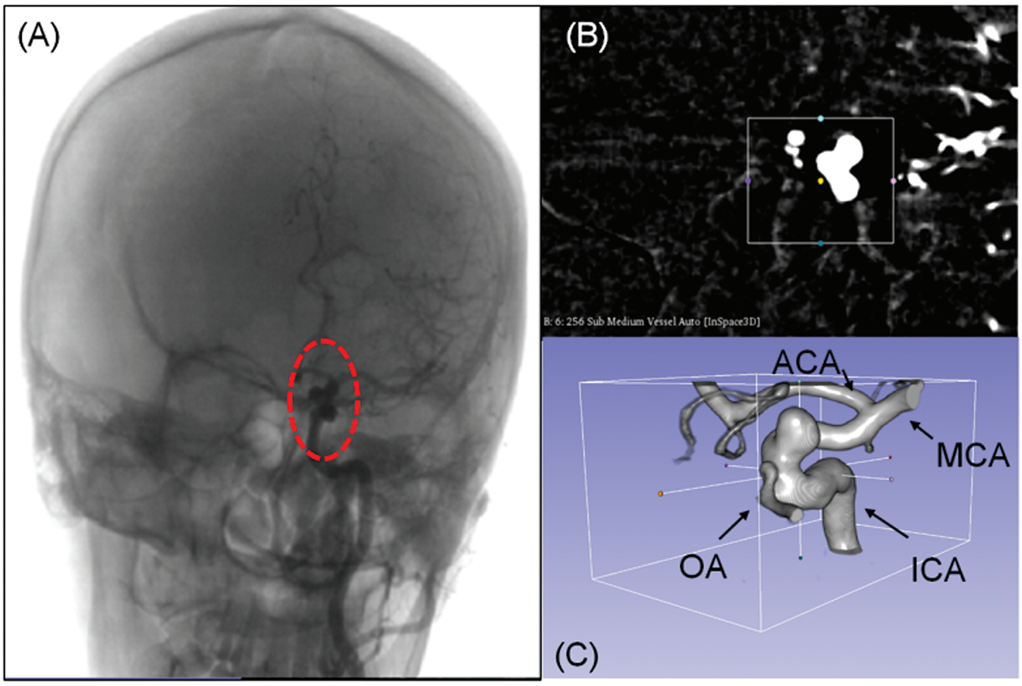

Fig. 1 A 59-year-old female patient's skull presentation with aneurysm sac shown with contrast fluid (**A**). Digital subtraction angiography (DSA) image of the patient's aneurysm sac on a plane (**B**). A three-dimensional rendered fluid domain of patient's aneurysm site at left internal carotid artery (LICA) with corresponding arteries, namely, anterior cerebral artery (ACA), middle cerebral artery (MCA), internal carotid artery (ICA), and ophthalmic artery (OA), labeled (**C**).

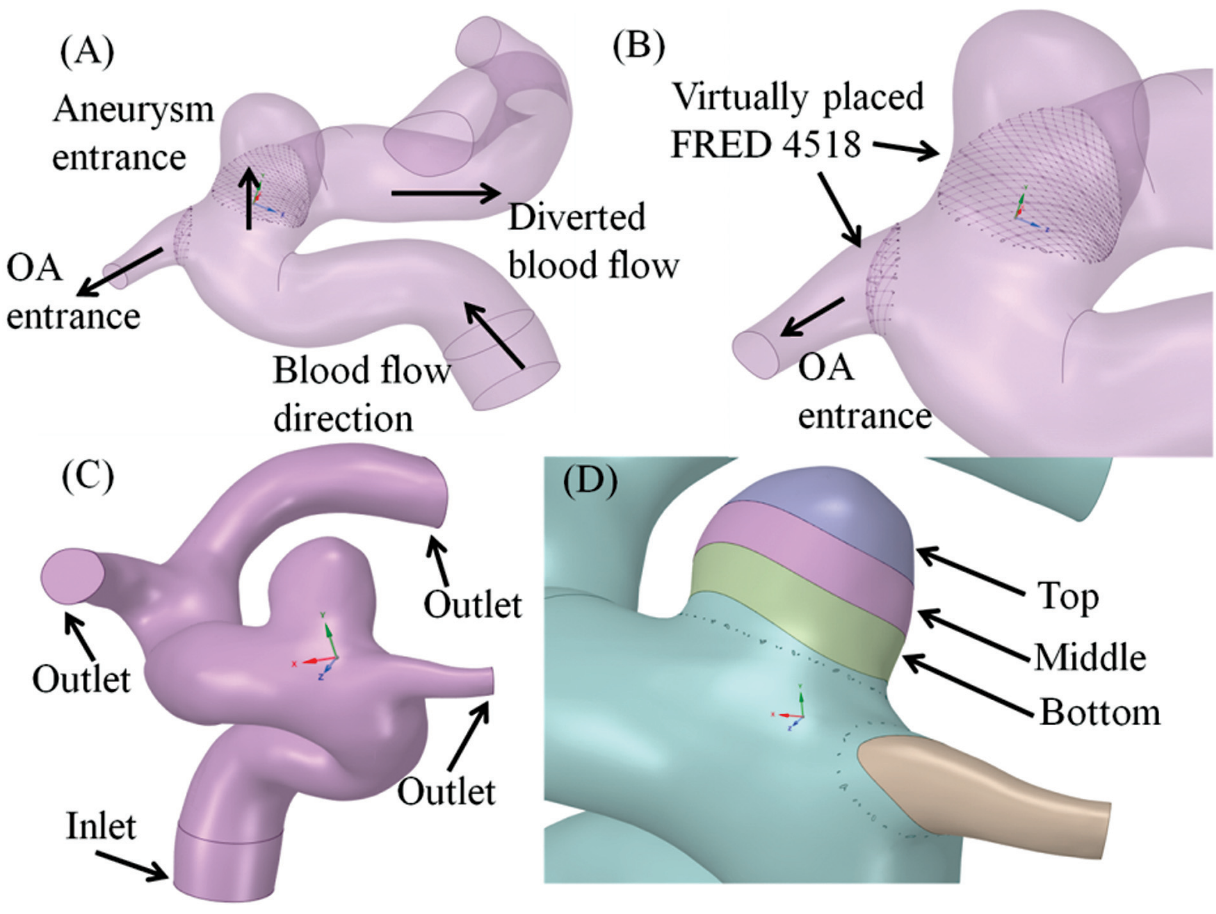

Fig. 2 Isometric view of virtually placed FRED4518 flow diverter (FD) stent at the patient's aneurysm neck (**A**). Enlarged view of the aneurysm neck with FRED4518 FD stent placement (**B**). The three-dimensional fluid domain of the patient's artery with an aneurysm (**C**). The aneurysm sac with three equal sections, namely, top, middle and bottom portions (**D**).

number of wires and wire diameters as FRED4518 is also considered in this work to understand better how two different models of the same FD with dissimilar porosity values perform at the aneurysm neck and OA entrance.

The mean diameter of the LICA, where the FD stent was implanted in the clinic, was measured by nearly 4 mm on the fluid domain built by DSA images. Therefore, FRED4518 and FRED4017 FD stents having 29 and 42% EMSA values obtained from MicroVention, Inc.[22] product catalog, respectively, based on the mean artery diameter were placed inside the 4-mm artery using a virtual stent deployment technique. However, EMSA values showed variation at the aneurysm neck being 24.6% (15% less than[22]) and 35% (nearly 17% less than[22]) for FRED4518 and 4017 FD stents, respectively, due to the nonuniform and curved structure of the parent artery. Similarly, EMSA values are calculated to be 21.2% (nearly 27% less than[22]) and 15% (almost 64% less than[22]) for FRED4017 FD and FRED4518 FD stents, respectively, at the inlet of the OA.

Boundary Conditions and Mesh Convergence

Blood in the artery was defined as Bird-Carreu non-Newtonian model with low and high shear viscosity values as 0.056 and 0.00345 Pa.s, respectively.[23,24] Blood density and molar mass were set to be 1047 kg/m^3 and 64.458 g/mol, respectively.[25] Womersley velocity profile[26,27] was employed in the artery inlet to accurately mimic the blood flow, while an 80 mm Hg pressure value was defined for all three outlets based on the patient's blood pressure, as shown in ►**Fig. 2C**. Time-dependent fluid flow simulations were run for three consecutive cardiac cycles (each cycle being 0.8 second long) based on the patient's heartbeat rate. Besides, the time step size was chosen to be 0.001 second and the numerical model was run 2,400 times to complete a total time of 2.4 seconds. The aneurysm sac was also split into three identical volume pieces, as illustrated in ►**Fig. 2D**, to identify the occlusion clearly, stagnated blood flow formation, and fluid flow characteristics in the sac.

Mesh convergence tests were performed by running the model with three different element numbers, namely, 20M, 26.7M, and 36.7M. Mainly, the relative error in mean viscosity was monitored, and simulations were continued until the relative error stayed under 5% inside the aneurysm sac. Therefore, the numerical model with 26.7M was decided to be used for simulations. Mesh placement at the LICA, OA, aneurysm neck, and sac region is shown in ►**Fig. 3A**, while the enlarged view of tetrahedral elements at the curved plane splitting the fluid domain into two pieces is also given in ►**Fig. 3B**.

Three of the patient-specific fluid domains of LICA with a giant aneurysm were prepared in the present study: no-stent, FRED4518, and FRED4017 FD stent-placed cases. Since the FD stent covers both the aneurysm neck and the OA, this study provided an exceptional opportunity to determine how much of the blood flow is diverted into the main artery and the OA entrance by the FD stents.

Results and Discussion

In the expanding field of neurointerventional surgery, CFD has emerged as a pivotal tool for understanding the complex hemodynamics within intracranial aneurysms and their alteration post-FD stent deployment. Many studies have harnessed CFD to simulate blood flow patterns, wall shear stress (WSS) distributions, and aneurysm occlusion processes, offering invaluable insights into the mechanics underlying successful aneurysm treatment. Therefore, patient-specific CFD modeling is a promising technique for predicting aneurysm occlusion post-FD deployment, underscoring the technique's potential in preoperative planning.[25,28] Besides, the impact of FD design variations on aneurysm hemodynamics, highlighting the intricate balance between device porosity and blood flow diversion efficacy, can directly affect the success of the treatment.[29] Despite these advancements, previous studies often grappled with limitations such as idealized aneurysm geometries, oversimplified

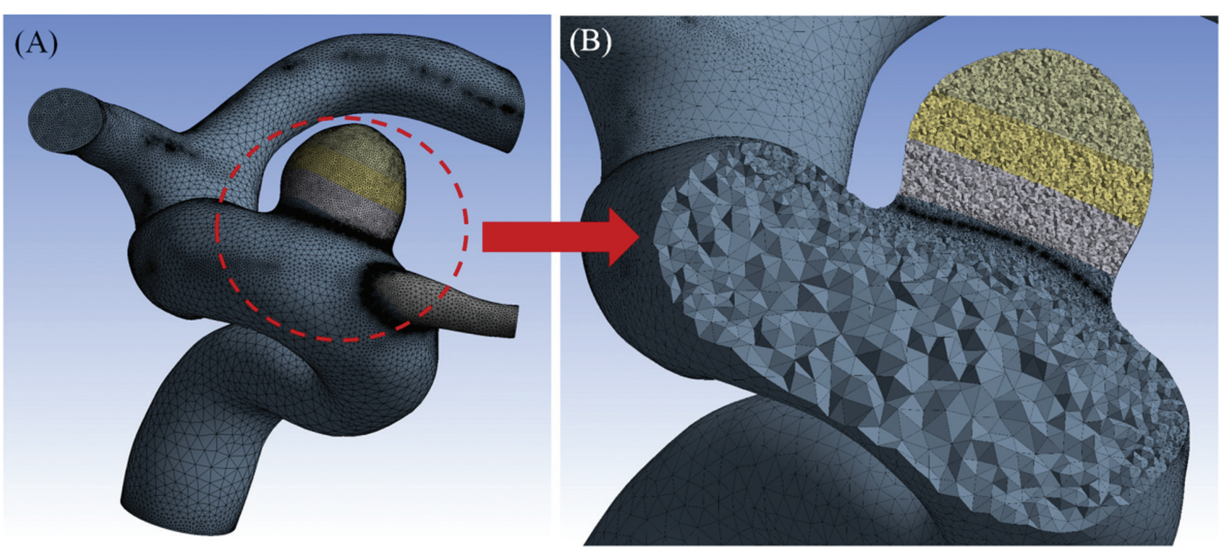

Fig. 3 Mesh placement at the computational domain (**A**). Enlarged view of cross-section obtained by a curved splitting plane (**B**).

blood rheology models, or neglect of physiological vessel wall motion and patient-specific blood flow conditions. Such constraints may affect the extrapolation of CFD findings to clinical practice, necessitating cautious interpretation and a judicious blend of computational insights with empirical clinical observations. Nevertheless, these contributions have scaffolded the foundation for ongoing research, driving the evolution of neurointerventional strategies toward more personalized, efficacious, and safer aneurysm management paradigms.

Investigation of Blood Flow Characteristics for No-Stent and Stent Cases

In the present study, DSA images obtained before (►**Fig. 4A**) and just after (►**Fig. 4C**) the FD stent placement in the clinic are compared with CFD simulation results (►**Fig. 4B, D**) for validation purposes. Velocity vectors obtained in CFD analysis are compared with the direction of the contrast fluid shown as black color pixels in the sac (►**Fig. 4A, C**) since the velocity vectors can provide an understanding of the blood flow orientation inside the aneurysm sac. It appears that blood flow can enter the aneurysm sac with a velocity higher than 0.5 cm/s before the stent placement by creating a large vortex structure (►**Fig. 4B**). However, once the FD is placed in the aneurysm neck, blood flow entering into the sac is incredibly retarded, emerging stagnation region formation near the aneurysm wall, as illustrated in ►**Fig. 4D**. Besides, nearly a 34% drop in mean velocity is observed between the top and bottom regions of the aneurysm for the stent case because FD absorbs most of the kinetic energy of the incoming blood flow. Therefore, blood flow immediately experiences deceleration in the occlusion region since the blood with low velocity shows considerable resistance to flow.

►**Fig. 5A** and **B** exhibits viscosity variations inside the patient's aneurysm sac for FRED4518 and FRED4017 FD stents, respectively. While the movement of contrast liquid can visualize the stagnation or occlusion region inside the sac, vorticity contour plots obtained from CFD simulations can indicate the formation of stagnation or occlusion region. Besides, stagnated contrast fluid accumulation in the aneurysm sac can be considered a successful stent deployment for the patient. Therefore, dynamic viscosity being the most relevant blood property for stagnation region formation, the mean dynamic viscosity in the aneurysm sac was increased by 46.4% more in the FRED4017 FD case compared with that of FRED4518. This is mainly because virtually implanted FRED4017 FD has a 10.4% higher EMSA value at the neck of the aneurysm than FRED4518 FD. It is noted that a 10.4% larger EMSA value FD caused a faster occlusion for FRED4017 FD, while FRED4518 FD provided a sufficient amount of blood to the OA and reduced the amount of blood entering into the aneurysm sac without creating an early stagnation in the aneurysm sac.

Effect of Flow Diverter Stents on Hemodynamics Inside of the Aneurysm Sac

FDs are designed to restrict blood circulation into the aneurysm; however, there is still debate among interventional

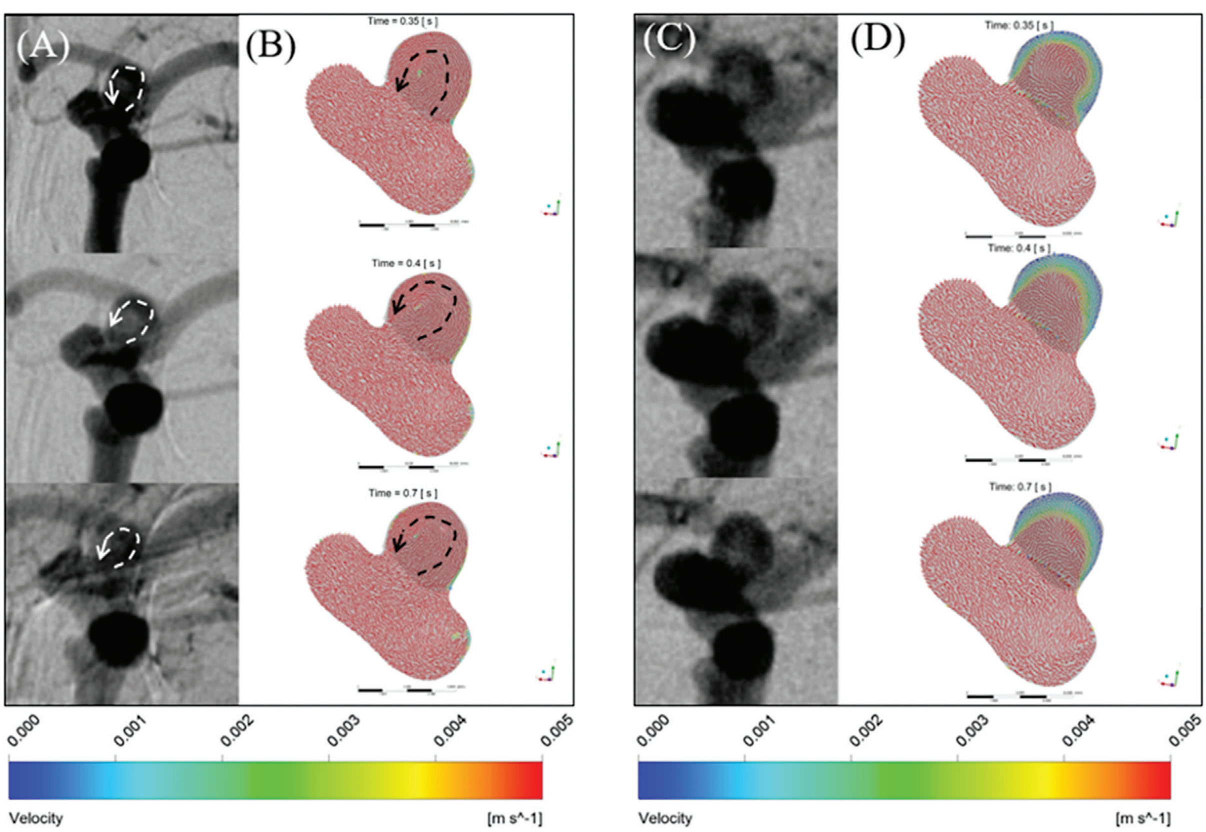

Fig. 4 Comparison of the digital subtraction angiography (DSA) images taken before (**A**) and just after the FRED4518 flow diverter (FD) placement (**B**) with computational fluid dynamics (CFD) analysis of the no-stent (**C**) and stent (**D**) cases.

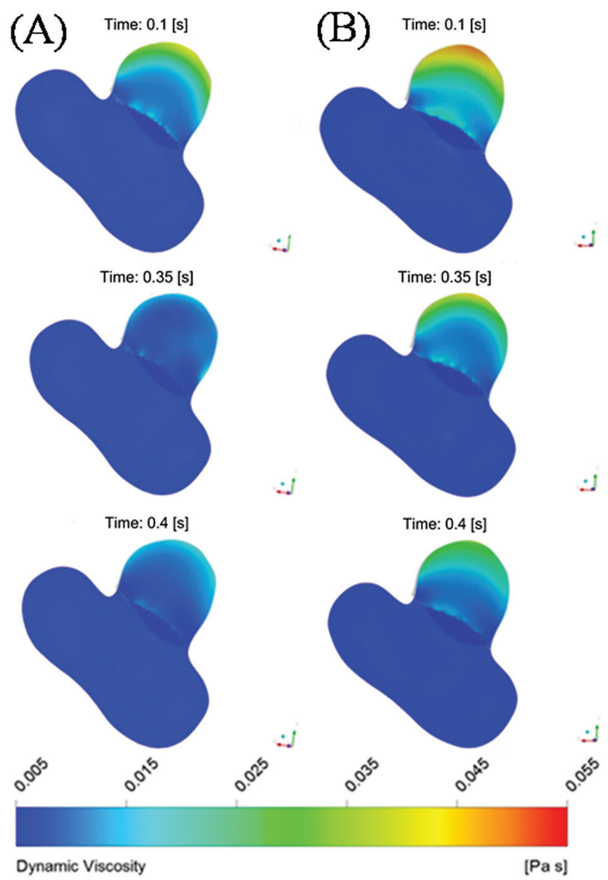

Fig. 5 Comparisons of the mean dynamic viscosity values of FRED4518 (**A**) and FRED4017 (**B**) flow diverter (FD) cases at the same time steps and on the same plane.

radiologists on the occlusion rate in the pouch. Besides, if an FD has to jail another artery during its placement to the aneurysm neck, hemodynamics at the aneurysm site becomes crucial. In such a case, the selection of FD plays a significant role since FD porosity should be small enough at the aneurysm neck to arrest most of the kinetic energy of blood flow, yielding a stagnation/occlusion region formation with a viscosity increase. Meanwhile, the porosity of the same FD should also be large enough to allow blood flow to the jailed artery to eliminate the possibility of a stroke or other fatal consequences.

In the present study, FRED4518 FD was placed at the patient's aneurysm neck, covering her OA as well in the clinic. It is noted that blood velocity values for FRED4518 FD cases were decreased by nearly 2,000, 780, and 410% (►**Fig. 5A**) and approximately 180, 80, and 90% (►**Fig. 5B**) increased in dynamic viscosity values at the top, middle, and bottom sections of the aneurysm sac, respectively, compared with no-stent case. Meanwhile, shear stress values show a drop of 1,210, 670, and 237% at the aneurysm sac's top, middle, and bottom sections, respectively. Besides, when FRED4518 FD is compared with FRED4017 FD, it is realized that FRED4017 FD caused 64.6, 44.6, and 30% larger mean dynamic viscosity values and 210, 140, and 98% smaller mean velocities to that of FRED4518 FD at the top, middle, and bottom of the sac, respectively. It is indicated that although FRED4017 with a high EMSA value could cause a complete occlusion quickly based on these fluid flow parameters, the jailed artery, namely, OA, of the patient could have suffered from insufficient incoming blood flow. Besides, sudden occlusion and a sharp decrease in shear stress inside the WSS can cause a cerebral hemorrhage.[30] It has also been documented that a

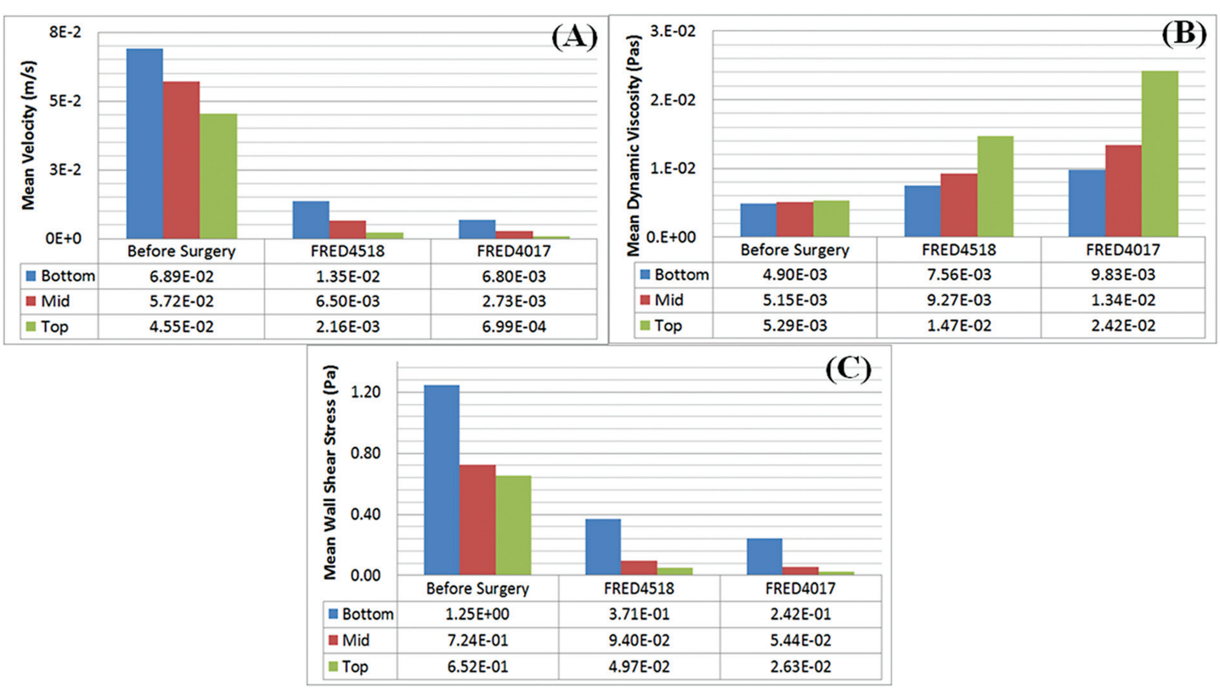

Fig. 6 Mean velocity (**A**), dynamic viscosity (**B**), and mean wall shear stress (**D**) inside the top, middle, and bottom of the aneurysm regions.

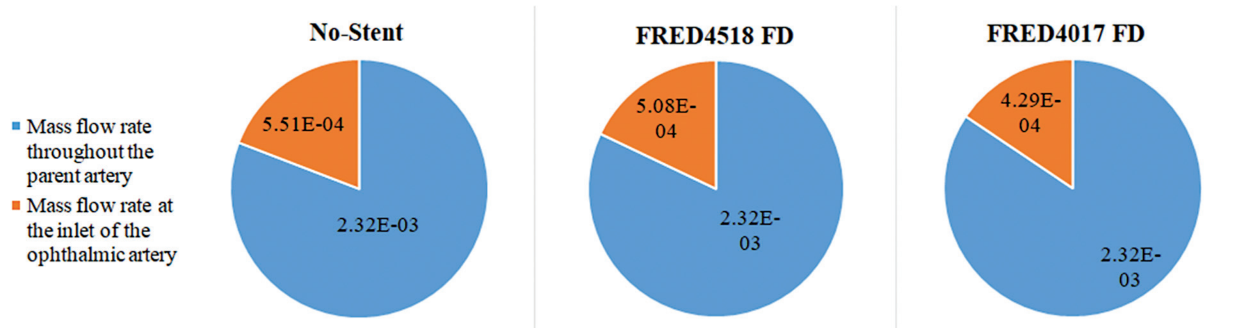

Fig. 7 Mass flow rates through the parent and the jailed arteries (i.e., ophthalmic artery [OA]) for no-stent, FRED4518 flow diverter (FD), and FRED4017 FD cases.

local decrease in WSS can be related to aneurysm rupture[31] (►**Fig. 6**).

Determination of the Flow Diversion Rate at the Aneurysm Site

Once an FD stent is placed into an aneurysm site, interventional radiologists monitor the amount of blood flow entering the aneurysm sac to determine the degree of occlusion in the pouch. However, when there is a jailed artery near the aneurysm site, the selection of FD can significantly affect the mass flow rate of the blood entering that jailed artery. Therefore, the blood's mass flow rate into the patient's OA was monitored in the present study. ►**Fig. 7** shows the amount of blood entering into the OA for the no-stent, FRED4518, and FRED4017 FD stent cases. FRED4518 and FRED4017 FD stents caused nearly 19.3 and 26.7% less blood flow in the OA compared with the no-stent case, respectively. Restriction of the blood flow in the OA can cause significant loss in the visual capacity of the patient. Since an FD stent creates an artificial occlusion at the inlet of the OA, the decreased blood flow at the OA is usually related to ocular ischemic syndrome (OIS). In those cases, patients can experience pain in the eye or loss of vision at various rates (mostly irreversible), and they are considered as symptoms of OIS. In the present study, the use of FRED4017 FD could cause nearly 40% more occlusion in the OA compared with the use of FRED4518. This means that consideration of only blood flow restriction into the aneurysm sac cannot be the most optimal and safe approach when there is a jailed artery at the aneurysm neck neighborhood.

In a subset of preceding CFD analyses, FD stents have been conceptualized as porous media, facilitating the examination of hemodynamic particles retained within the aneurysmal sac.[25,29,32,33] Concurrently, an empirical correlation has been formulated to approximate regions of stagnated flow within the sac.[34] While the porous media paradigm offers insights into the hemodynamic environment proximal to the aneurysm, the present investigation distinguishes itself by simulating the deployment of the FD stent within the aneurysmal sac, thereby enabling direct observation of blood flow through and around the stent struts.

Nevertheless, it is imperative to recognize certain constraints inherent to our methodology. Primarily, the principal artery and aneurysm were presumed to be nondeformable entities; secondarily, the influence of anticoagulant usage[35] was not incorporated within our computational model. Lastly, the generalizability of our findings may be circumscribed by the singular patient profile utilized, although this approach does permit an in-depth analysis of FD selection effects in the context of an encased OA.

While the present study acknowledges that the virtual environment may not fully replicate the complexities of in vivo conditions, this modeling approach does provide a controlled setting to isolate and examine specific variables of interest. In this case, the virtual deployment allows for a detailed analysis of the hemodynamic changes induced by FDs with varying EMSA values, which might be more challenging to distinguish in a clinical setting due to many confounding factors. To address this point, the virtual stent deployment model allows for a focused examination of the "jailing" effect and its potential consequences on the OA, which is supported by the observed complication in a patient. This approach underscores the predictive value of patient-specific CFD modeling in assessing the risks associated with different FD stents, thereby contributing valuable insights to the preoperative planning process.

The intersection of CFD insights and clinical neurosurgery has opened new avenues for tailoring interventional strategies to individual patient profiles, particularly in managing aneurysms near critical structures like the OA. Our findings elucidate the nuanced relationship between FD deployment and the risk of OIS, a severe complication stemming from compromised OA blood flow. However, the clinical applicability of these insights extends beyond immediate procedural outcomes, urging a deeper exploration of long-term patient well-being. Recognizing that aneurysm geometry and hemodynamic patterns play pivotal roles in postprocedural recovery, it becomes imperative to integrate patient-specific vessel architecture and flow dynamics into preoperative planning. This approach enhances the predictive accuracy of potential OIS risk and facilitates the design of FDs optimized for individual anatomical variations, thereby mitigating long-term adverse effects. Future research should thus prioritize longitudinal studies that combine CFD modeling with empirical clinical data, aiming to refine our understanding of how procedural interventions translate into durable patient outcomes. By doing so, we move closer to a paradigm where neurointerventional surgery is as personalized as it is precise, maximizing therapeutic benefits while minimizing the risk of complications such as OIS.

Conclusion

In the present study, the ophthalmic segment of a 59-year-old female patient's LICA was jailed during the implantation of FRED4518 FD into the aneurysm site in the clinic. FRED4017 FD was also virtually knitted inside the aneurysm site by using a stent deployment method to reveal the hemodynamic differences at the patient's aneurysm sac and OA entrance. CFD results indicated that FRED4017 had a larger EMSA value than FRED4518, caused nearly total occlusion inside the aneurysm sac, and blocked 40% more blood flow into jailed OA. This could yield the possibility of an OIS. Therefore, using FRED4017 for this patient may seem to be the proper treatment for the aneurysm. At the same time, the FD with a high EMSA value can lead to a significant viscosity increase and focal low WSS areas in the aneurysm sac, which increases the risk of delayed aneurysm rupture.[36,37] Besides, when the patient is symptomatic and hypertensive, multiple risk factors may develop for the late aneurysm rupture.[37] Although the additional coiling might be applied in the case of residual aneurysmal filling, it was decided to proceed with a small EMSA value FRED4518 FD stent because higher EMSA values are associated with an increased risk of jailing, potentially leading to ischemic complications for the studied numerical models. Therefore, early stagnation was not observed in the images obtained after the FD deployment in the same session. However, total aneurysmal occlusion was observed in the third month of cranial arterial MR angiography. Besides, no recurrence was detected in the 6th month, 1 year, and 2 years of control MR angiographies. The patient's complaints completely disappeared in the 6th month of treatment. There were no complications related to the procedure. In conclusion, consideration of only blood flow restriction into the aneurysm sac cannot be the most optimal and safest approach when there is a jailed artery at the aneurysm neck neighborhood.

Conflict of Interest
None declared.

References

1 Lv X, Yang H, Liu P, Li Y. Flow-diverter devices in the treatment of intracranial aneurysms: a meta-analysis and systematic review. Neuroradiol J 2016;29(01):66–71
2 Iancu D, Lum C, Ahmed ME, et al. Flow diversion in the treatment of carotid injury and carotid-cavernous fistula after transsphenoidal surgery. Interv Neuroradiol 2015;21(03):346–350
3 Lanzino G, Crobeddu E, Cloft HJ, Hanel R, Kallmes DF. Efficacy and safety of flow diversion for paraclinoid aneurysms: a matched-pair analysis compared with standard endovascular approaches. AJNR Am J Neuroradiol 2012;33(11):2158–2161
4 Chalouhi N, Tjoumakaris S, Starke RM, et al. Comparison of flow diversion and coiling in large unruptured intracranial saccular aneurysms. Stroke 2013;44(08):2150–2154
5 Zanaty M, Chalouhi N, Starke RM, et al. Flow diversion versus conventional treatment for carotid cavernous aneurysms. Stroke 2014;45(09):2656–2661
6 Piano M, Lozupone E, Milonia L, et al. Flow diverter devices in the treatment of complex middle cerebral artery aneurysms when surgical and endovascular treatments are challenging. J Stroke Cerebrovasc Dis 2022;31(12):106760
7 Abdelkhalek H, Abdelhameed EA, Zakarea A, El Malky I. Predictors of flow diverter stent in large and giant unruptured intracranial aneurysms, single-center experience. Neurol Sci 2022;43(11): 6399–6405
8 Lee ITL, Kao Y-S, Lai Y-J, Yen H-H. Flow diverter retreatment for intracranial aneurysms: a meta-analysis of efficacy and feasibility. Interv Neuroradiol 2024;30(01): 37–42
9 Hanel RA, Kallmes DF, Lopes DK, et al. Prospective study on embolization of intracranial aneurysms with the pipeline device: the PREMIER study 1 year results. J Neurointerv Surg 2020;12 (01):62–66
10 Meyers PM, Coon AL, Kan PT, Wakhloo AK, Hanel RA. SCENT trial. Stroke 2019;50(06):1473–1479
11 Pierot L, Spelle L, Berge J, et al. SAFE study (Safety and efficacy Analysis of FRED Embolic device in aneurysm treatment): 1-year clinical and anatomical results. J Neurointerv Surg 2019;11(02): 184–189
12 Giorgianni A, Agosti E, Molinaro S, et al. Flow diversion for acutely ruptured intracranial aneurysms treatment: a retrospective study and literature review. J Stroke Cerebrovasc Dis 2022;31 (03):106284
13 Simgen A, Roth C, Kulikovski J, et al. Endovascular treatment of unruptured intracranial aneurysms with flow diverters: a retrospective long-term single center analysis. Neuroradiol J 2023;36 (01):76–85
14 Kaiser DPO, Boulouis G, Soize S, et al; Compressive Aneurysm Study Group. Flow diversion for ICA aneurysms with compressive neuro-ophthalmologic symptoms: predictors of morbidity, mortality, and incomplete aneurysm occlusion. AJNR Am J Neuroradiol 2022;43(07):998–1003
15 Burrows AM, Brinjikji W, Puffer RC, Cloft H, Kallmes DF, Lanzino G. Flow diversion for ophthalmic artery aneurysms. AJNR Am J Neuroradiol 2016;37(10):1866–1869
16 Charbonnier G, Desilles J-P, Escalard S, et al. Timing and spectrum of neurological complications after flow diverter implantation for intracranial aneurysms. Front Neurol 2021; 12:590383
17 Tanaka Y, Nagatsuka H, Miki Y, et al. Two patients of visual disturbance and optic perineuritis after placement of a flow diverter. Radiol Case Rep 2022;17(05):1487–1490
18 Kato Y, Kimura N, Endo H, et al. Visual Impairment due to a large paraclinoid aneurysm treated with parent artery occlusion and bypass: a case report. J Stroke Cerebrovasc Dis 2022;31(04): 106280
19 Xu C, Wu P, Sun B, et al. Incomplete occlusion and visual symptoms of peri-ophthalmic aneurysm after treatment with a pipeline embolization device: a multi-center cohort study. Acta Neurochir (Wien) 2022;164(08):2191–2202
20 Rouchaud A, Leclerc O, Benayoun Y, et al. Visual outcomes with flow-diverter stents covering the ophthalmic artery for treatment of internal carotid artery aneurysms. AJNR Am J Neuroradiol 2015;36(02):330–336
21 Touzé R, Gravellier B, Rolla-Bigliani C, et al. Occlusion rate and visual complications with flow-diverter stent placed across the ophthalmic artery's origin for carotid-ophthalmic aneurysms: a meta-analysis. Neurosurgery 2020;86(04): 455–463
22 I. MicroVention Terumo, No Title, içinde: Flow Re-Direction Endoluminal Device,. 2015: ss. 1–2. Accessed June 15, 2024 at: https://www.microvention.com/products/fred-family
23 Jahangiri M, Saghafian M, Sadeghi MR. Effects of non-Newtonian behavior of blood on wall shear stress in an elastic vessel with simple and consecutive stenosis. Biomed Pharmacol J 2015; 8:123–131

24 Hippelheuser JE, Lauric A, Cohen AD, Malek AM. Realistic non-Newtonian viscosity modelling highlights hemodynamic differences between intracranial aneurysms with and without surface blebs. J Biomech 2014;47(15):3695–3703
25 Mutlu O, Olcay AB, Bilgin C, Hakyemez B. Evaluating the effectiveness of 2 different flow diverter stents based on the stagnation region formation in an aneurysm sac using Lagrangian coherent structure. World Neurosurg 2019;127:e727–e737
26 Womersley JR. Method for the calculation of velocity, rate of flow and viscous drag in arteries when the pressure gradient is known. J Physiol 1955;127(03):553–563
27 Pashaei A, Fatouraee N. An analytical phantom for the evaluation of medical flow imaging algorithms. Phys Med Biol 2009;54(06): 1791–1821
28 Mutlu O, Salman HE, Yalcin HC, Olcay AB. Fluid flow characteristics of healthy and calcified aortic valves using three-dimensional Lagrangian coherent structures analysis. Fluids (Basel) 2021;6:203
29 Mutlu O, Olcay AB, Bilgin C, Hakyemez B. Understanding the effect of effective metal surface area of flow diverter stent's on the patient-specific intracranial aneurysm numerical model using Lagrangian coherent structures. J Clin Neurosci 2020;80:298–309
30 Cebral JR, Mut F, Weir J, Putman C. Quantitative characterization of the hemodynamic environment in ruptured and unruptured brain aneurysms. AJNR Am J Neuroradiol 2011;32(01):14515–1
31 Zhou G, Zhu Y, Yin Y, Su M, Li M. Association of wall shear stress with intracranial aneurysm rupture: systematic review and meta-analysis. Sci Rep 2017;7(01):5331
32 Mutlu O, Olcay AB, Bilgin C, Hakyemez B. Evaluating the effects of the wire number of flow diverter stents on the non-stagnated region formation in an aneurysm sac using Lagrangian coherent structure and hyperbolic time analysis. World Neurosurg 2020; 133:e666–e682
33 Mutlu O, Olcay AB, Bilgin C, Hakyemez B. Evaluating the effect of the number of wire of flow diverter stents on the nonstagnated region formation in an aneurysm sac using Lagrangian coherent structure and hyperbolic time analysis. World Neurosurg 2020; 133:e666–e682
34 Altındağ B, Bahadır Olcay A, Furkan Tercanlı M, Bilgin C, Hakyemez B. Determining flow stasis zones in the intracranial aneurysms and the relation between these zones and aneurysms' aspect ratios after flow diversions. Interv Neuroradiol 2023; 159101992311628:15910199231162878
35 Tercanlı MF, Olcay AB, Mutlu O, Bilgin C, Hakyemez B. Investigation of the effect of anticoagulant usage in the flow diverter stent treatment of the patient-specific cerebral aneurysm using the Lagrangian coherent structures. J Clin Neurosci 2021; 94:86–93
36 Turowski B, Macht S, Kulcsár Z, Hänggi D, Stummer W. Early fatal hemorrhage after endovascular cerebral aneurysm treatment with a flow diverter (SILK-Stent): do we need to rethink our concepts? Neuroradiology 2011;53(01):37–41
37 Kulcsár Z, Houdart E, Bonafé A, et al. Intra-aneurysmal thrombosis as a possible cause of delayed aneurysm rupture after flow-diversion treatment. AJNR Am J Neuroradiol 2011;32(01):20–25

